Eidgenössische Technische Hochschule Zürich
Swiss Federal Institute of Technology Zurich

Numerical simulations of parasitic folding in multilayers

Marcel Frehner and Stefan M. Schmalholz
Department of Earth Science, ETH Zurich, 8092 Zurich, Switzerland, marcel.frehner@erdw.ethz.ch, +41 44 632 88 72

Abstract

We use the finite element method to simulate slow viscous (Newtonian) flow in two dimensions without gravity and to model asymmetric (S- and Z-shaped) and symmetric (M-shaped) parasitic folds during multilayer folding. During multilayer folding, the matrix between stiffer layers shows a deformation close to pure shear in the hinge area and a combination of pure and simple shear in the limb areas. Thinner layers placed between thicker layers develop symmetric parasitic folds in the hinge, and eventually asymmetric parasitic folds in the limbs of the larger fold. Our results verify numerically the theory that asymmetric parasitic folds develop from symmetric buckle-folds that are sheared by the relative displacement of the thick layers in the limbs of the first-order fold. To develop asymmetric shapes, the amplitudes of the parasitic folds must exceed a critical value before the first-order fold begins to amplify. Otherwise the parasitic folds are unfolded during flattening that takes place in the limb area between the thick layers. More than five thin layers are necessary to generate distinct asymmetric parasitic folds for the applied model setting. More layers generate higher amplification rates in the thin layers and, hence, higher amplitudes.

Figure 1: Big scale multilayer fold with symmetric and asymmetric parasitic folds in the Makran area, Southern Iran. With of picture is approx. 500m.

Figure 2: Asymmetric, S- and Z-shaped, parasitic folds in folded, foliated metagabbros, Val Malenco, Southern Swiss Alps (picture courtesy of Jean-Pierre Burg).

Please help yourself

Two-layer folds

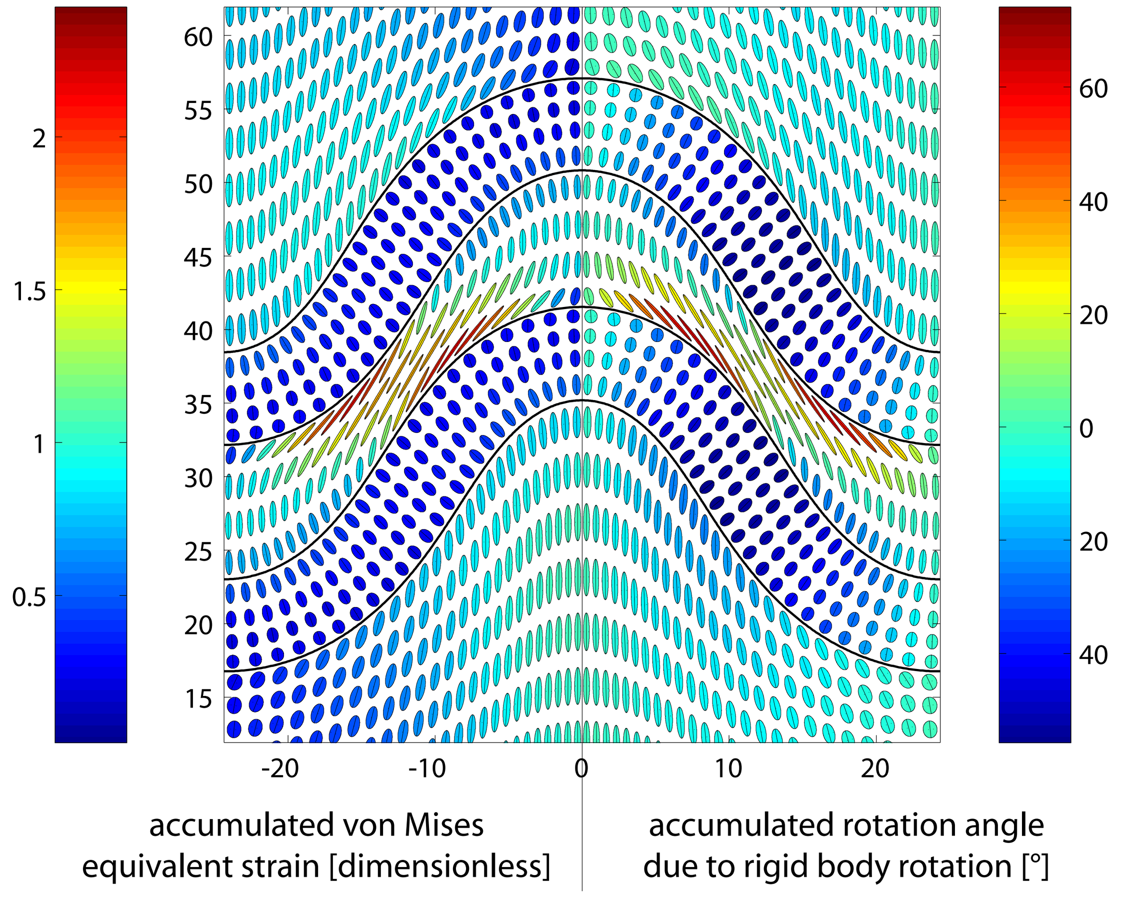

Figure 3: Two folded viscous layers after 40% bulk shortening. Viscosity contrast between layers and matrix is 100. Initial spacing of layers is equal to layer thickness. Strain ellipses are coloured with accumulated strain and finite rotation angle, respectively.

The matrix between a two-layer fold can be divided into three regions of different deformation paths:

(i) Near the hinge: Layer-parallel shortening during the whole folding history, total strain can be approximated by pure shear.
(ii) Near the inflexion point: Layer-parallel shortening, followed by layer-parallel shearing and flattening normal to the layer.
(iii) Transition zone between (i) and (ii) the two regions of deformation interfere.

The deformation path of region (ii) consists of three main phases:

1) Layer-parallel shortening: Occurs before the onset of buckling of the two stiff layers.
2) Layer-parallel shearing: Initial buckling of the two stiff layers causes a simple-shear-type deformation.
3) Flattening normal to the layer: Increased amplification of the stiff layers leads to a flattening of the matrix.

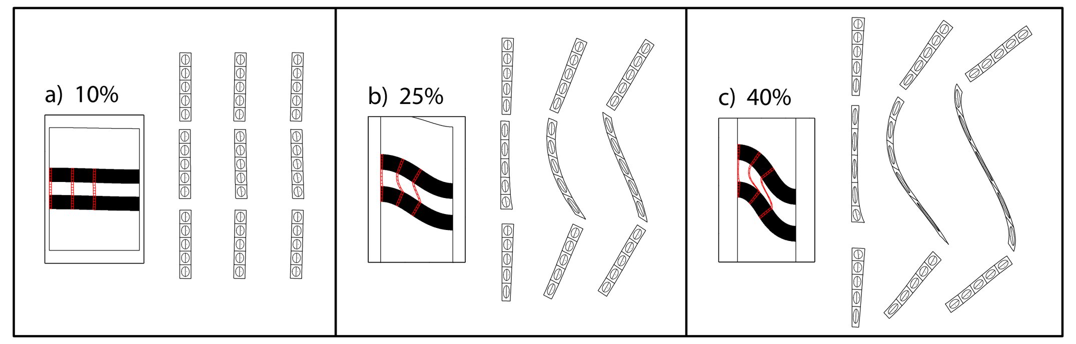

Figure 4: Finite strain evolution for two folded layers. Each red beam initially consisted of five squares. The red beams are magnified on right hand side and drewn with finite strain ellipses. Three regions of deformation in the matrix between the two layers are deformed differently. The beam between the limbs develops a S-shape while the one in the transition zone develops a tail-shape. The initial layer-parallel shortening is visible in all beams in the matrix at 10% bulk shortening but continues at the fold hinge only.

Multilayer folds

The three deformation phases for the matrix near the inflexion point of a two-layer system can be reformulated:

1) Layer-parallel shortening; no buckling of the thick layers; thin layers start to buckle and build symmetric fold arrays (gray lines in figure 6a)
2) Buckling of thick layers causes shearing in between; folds of the multilayer stack become asymmetric
3) Increased amplification of thick layers leads to flattening normal to the layers; amplitudes of the thin layers are reduced and some disappear

Selection of the fold arrays that outlast the third phase is due to their amplitude at the onset of buckling of the thick layers. Amplification rates of thin layers depend on the number of layers. A higher number of layers amplify faster and chances to outlast the flattening phase are higher.

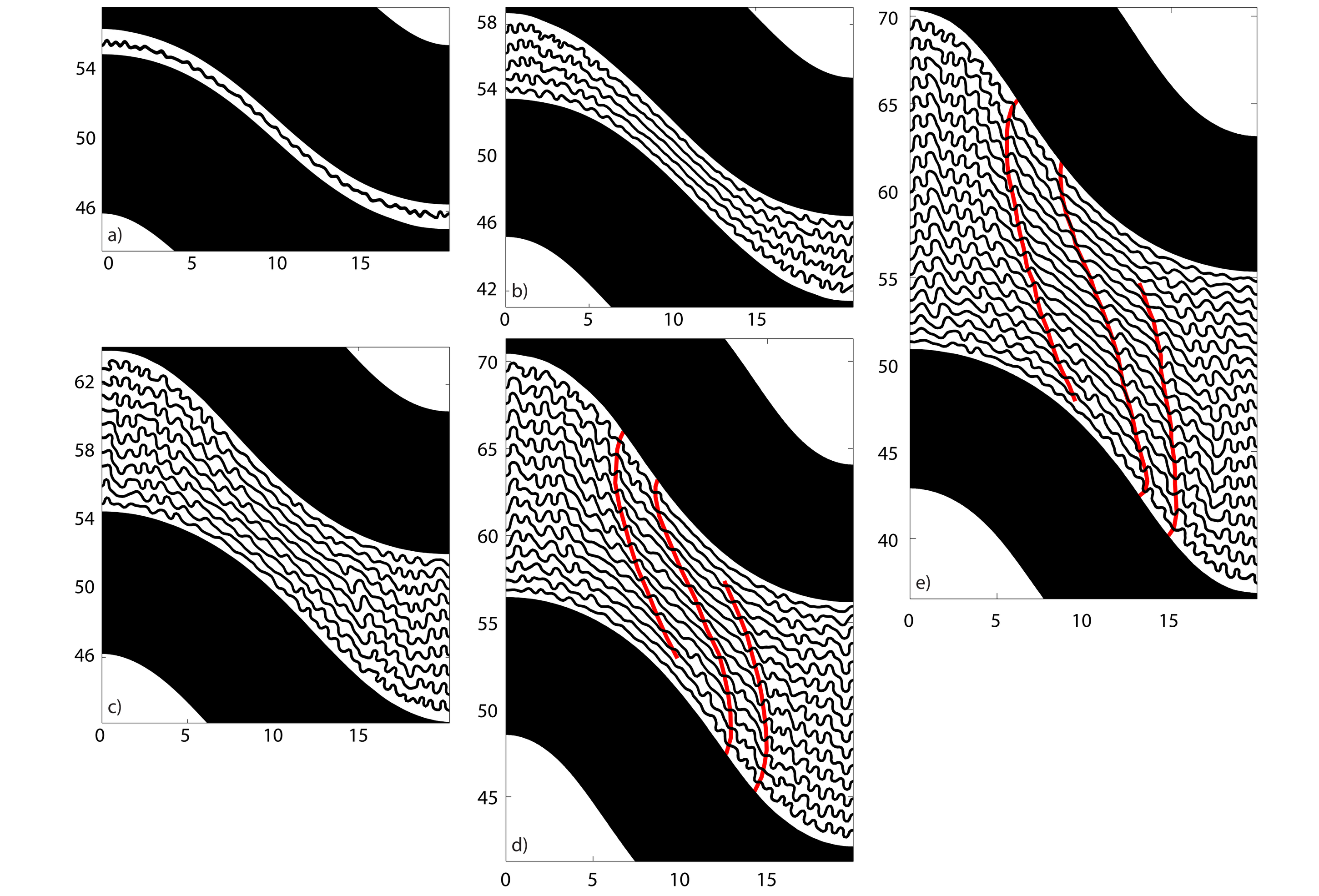

Figure 5: a) to e): Geometry of five different multilayer models after 50% bulk shortening. The models only differ in the number of thin layers between the two thick layers. Red lines connect parasitic folds that were vertically stacked in the initial folding stage.

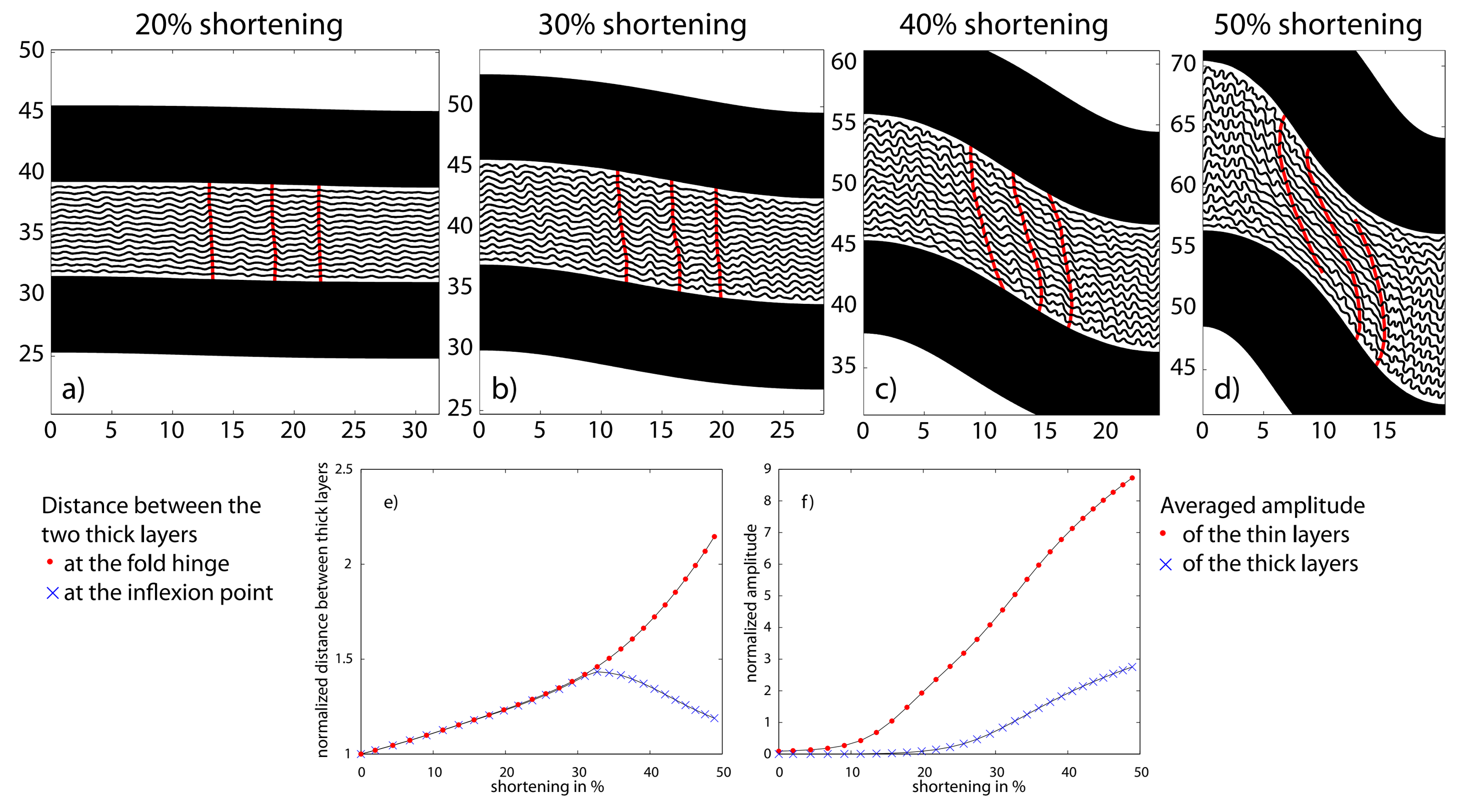

Figure 6: a) to d) Four stages of deformation of a multilayer stack with 15 thin layers. Red lines connect parasitic folds that were vertically stacked in the initial folding stage a). These lines develop shapes that look very simmilar to the two-layer case (Figure 3)
e) Line with red dots: Evolution of distance between the two thick layers in the hinge, normalized by the initial distance between the thick layers. Line with blue crosses: Evolution of minimum distance between the two thick layers, which occurs between the two inflexion points. This evolution of layer distances is very similar to the case without thin layers between the thick layers. **f)** Line with red dots: Evolution of the average amplitude of the thin layers in the hinge zone of the large scale fold, normalized with the initial thickness of the thin layers. Line with blue crosses: Average amplitude of the thick layers, normalized with their initial thickness.

Discussion

Comparison between figures 4 and 6 suggest that the fold arrays that are vertically stacked at the initial deformation phase (figure 6a) deform passively thereafter.

Performing exactly the same simulation with and without a multilayer stack between the two thick layers shows that the deformation of the thick layers is barely dependent on the presence of the thin layers. In other words the thin layers do not influence the deformation of the thick layers, which means that the thin layers deform passively between the thick layers.

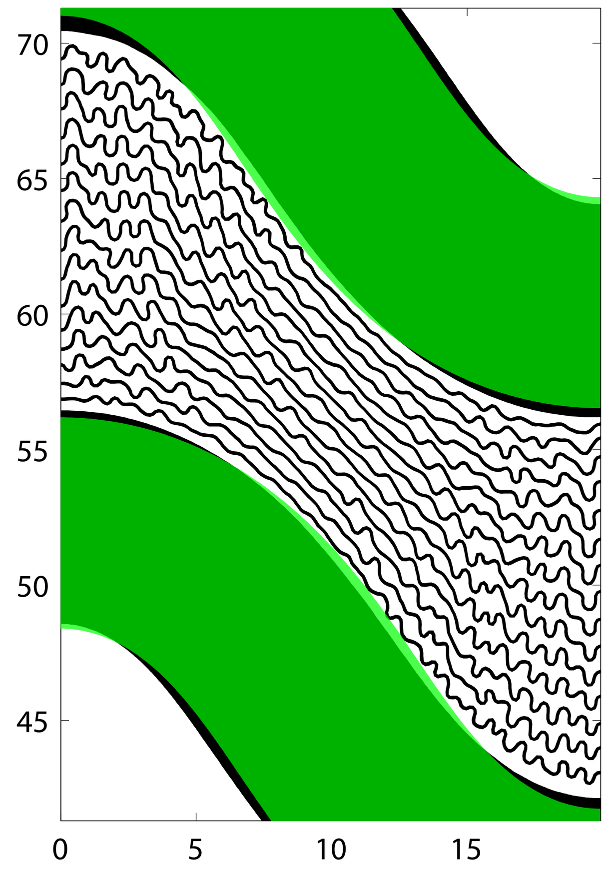

Figure 7: Two simulations are drawn on top of each other for comparison. The black layers show the folded multilayer system with 15 thin layers after 50% bulk shortening. The two transparent green layers (also 50% bulk shortening) exhibited the same initial conditions than the thick black layers, but without thin layers in between.

Application to a more complex geometry

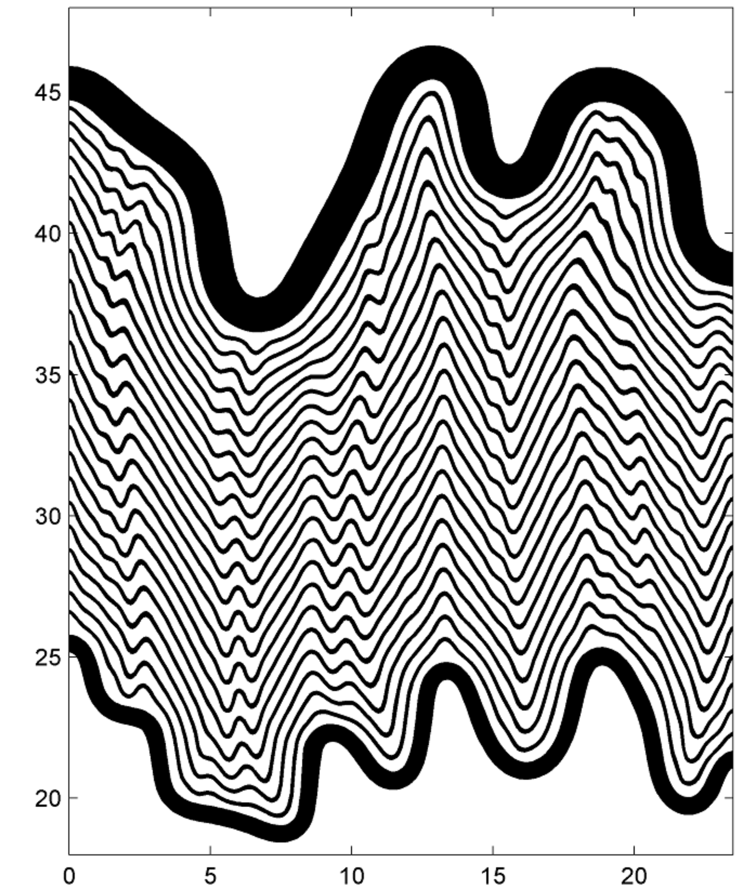

Figure 8: Numerical simulation of parasitic folding for more complex geometries and 22 thin layers after 53% bulk shortenig. The viscosity contrast between stiff layers and matrix is 100. The two external layers have a different thickness and initially had a bell-shaped perturbation of the layer interface. The thin layers had initially a random perturbation. The folds in the external layers have different wavelengths due to their different thickness. The simulation shows both S- and Z-shaped asymmetric, and M-shaped symmetric parasitic folds. The thin layer located above the lowest layer shows hinge collapse structures at the convex upwards fold hinges.

Conclusions

- Numerical simulations verified Ramberg's (1963) theory of parasitic fold development for Newtonian materials. Asymmetric parasitic folds originate from symmetric buckle folds that are sheared into an asymmetric shape by the relative displacement between the thick layers.
- The relative timing between the amplification of the parasitic and the larger folds strongly controls the development of asymmetric folds in the limb zone of the larger fold. If the larger fold amplifies while the parasitic folds still have small amplitudes, early buckles are unfolded by the flattening between the thick layers. In contrast, symmetric parasitic folds in the hinge zone always develop because the deformation is there dominantly pure shear.
- A larger numbers of thin layers favours the development of asymmetric parasitic folds, because a large number of thin layers has a larger amplification.
- The application to a more complex numerical setup shows parasitic fold geometries and other features close to nature.

Reference

Ramberg, H. 1963. Evolution of drag folds.Geological Magazine 100(2), 97-110.